

1 **Excitation of Delocalized Long-Lived States of Aliphatic Protons**  
2 **at Low and High Magnetic Fields**

3  
4 Sebastiaan Van Dyck, Coline Wiame, Kirill F. Sheberstov\* and Geoffrey Bodenhausen

5  
6  
7 Chimie Physique et Chimie du Vivant (CPCV, UMR 8228), Département de Chimie,  
8 École Normale Supérieure, PSL University, Sorbonne Université,  
9 75005 Paris, France

10  
11  
12 \*Corresponding Author:

13 Dr Kirill Sheberstov email: [kirill.sheberstov@ens.psl.eu](mailto:kirill.sheberstov@ens.psl.eu)

14  
15 To be submitted to Magn. Reson. (Groupement Ampere)

16  
17 *SVD's ORCID: 0009-0005-7622-5753*

18 *KS's ORCID: 0000-0002-3520-6258*

19 *GB's ORCID: 0000-0001-8633-6098*

20 *CW ORCID: 0009-0008-3517-3354*

21

22

## Abstract

23 Long-lived states (LLS) can be excited in geminal protons of aliphatic chains by mono- or  
24 poly-chromatic spin-lock induced crossings (SLIC), i.e., by application of one or more  
25 selective radio-frequency (RF) fields to create delocalised population imbalances between  
26 states belonging to different symmetry under spin permutations. At low fields (in this work at  
27 1.4 T, or 60 MHz for proton NMR), these experiments are challenging due to the proximity of  
28 the chemical shifts and the need to consider the full untruncated  $J$ -coupling Hamiltonian. Five  
29 molecules were studied in this work: ethanolamine, lysine, vitamin B1, metronidazole, and  
30 phenoxyethylamine (POEA). For POEA and metronidazole, the LLS are reported for the first  
31 time. Measurements were carried out at low and high magnetic fields (1.4 T and 11.7 T, or 60  
32 and 500 MHz for protons) using 60 MHz Magritek and 500 MHz Bruker NEO spectrometers.  
33 The rates  $R_{LLS} = 1/T_{LLS}$  and  $R_1 = 1/T_1$  were determined using monochromatic SLIC excitation  
34 at both fields. We describe strategies for optimising SLIC conditions in cases where the signals  
35 of neighbouring  $\text{CH}_2$  groups are relatively close to each other.

36

37

## Key words

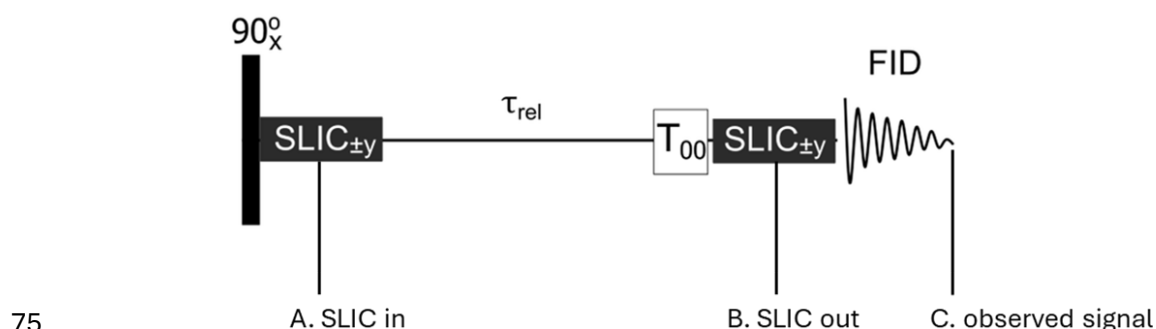
38 Long-lived states; Field-dependent relaxation; Spin-lock induced crossings.

39

41 A long-lived state (LLS) is a nuclear spin state that has a lifetime longer than the longitudinal  
 42 relaxation time [Carravetta et al., 2004]. Usually, an LLS corresponds to an imbalance between  
 43 states with different spin permutation symmetries [Stevanato et al., 2015, Sheberstov et al.,  
 44 2019a, Sabba et al. 2022]. In an isolated two-spin system with two protons  $H_A$  and  $H_{A'}$ , such  
 45 an imbalance can occur between the average population of three symmetric triplet states ( $|T_1\rangle$ ,  
 46  $|T_0\rangle$ ,  $|T_{-1}\rangle$ ) and the population of the singlet state ( $|S_0\rangle$ ), which is antisymmetric under spin  
 47 permutation. The resulting population imbalance is immune to relaxation due to the dipole-  
 48 dipole coupling between the two protons  $H_A$  and  $H_{A'}$ , thus resulting in a long-lived state. In  
 49 short *achiral* aliphatic chains  $-(CH_2-CH_2)-$  with 4 protons, the geminal proton pairs are  
 50 chemically equivalent because of the lack of stereogenic centers, but they can be magnetically  
 51 inequivalent provided each  $CH_2$  group has a distinct chemical shift and provided the vicinal  
 52 scalar couplings between neighbouring  $CH_2$  groups differ. This occurs if the populations of the  
 53 rotamers that result from rotations about the C-C bond are *not* equal, so that the differences  
 54 between the vicinal couplings  $\Delta J = J_{AX} - J_{AX'} = J_{A'X} - J_{A'X'}$  do not vanish. Magnetic  
 55 inequivalence allows one to excite an LLS that is *delocalized* across the two  $AA'$  and  $XX'$  spin  
 56 pairs. This can be achieved by mono- or poly-chromatic spin-lock induced crossings (SLIC)  
 57 [DeVience et al., 2013, Sonnefeld et al., 2022a, Sonnefeld et al., 2022b], i.e., by application of  
 58 one or two selective radio-frequency (RF) fields simultaneously. Although long-lived state  
 59 excitation can alternatively, also be achieved via Adiabatic-Passage Spin Order Conversion  
 60 (APSOC, [Pravdivtsev et al., 2016]), this work focuses exclusively on SLIC-based excitation  
 61 methods. This paper focuses on mono-chromatic SLIC excitation solely. At high fields (e.g.  
 62 500 MHz), the RF amplitude for single quantum (SQ) conditions, must be  $v_{SLIC}^{SQ} = 2J_{intra}$ ,  
 63 where  $J_{intra}$  is an averaged value of the intrapair couplings between geminal protons, e.g.  
 64  $J_{intra} = \frac{1}{2}\{ {}^2J(H_A, H_{A'}) + {}^2J(H_X, H_{X'})\}$ . A pulse duration  $\tau_{SLIC}^{SQ} = 1/(|\sqrt{2}\Delta J|)$  suffices for SQ  
 65 level-anti-crossing (LAC). After a variable relaxation delay  $\tau_{rel}$ , one applies a  $T_{00}$  filter which  
 66 removes all terms other than the desired population imbalance [Tayler et al., 2020]. A second  
 67 SLIC pulse then reconverts the LLS into observable magnetisation (Fig. 1).

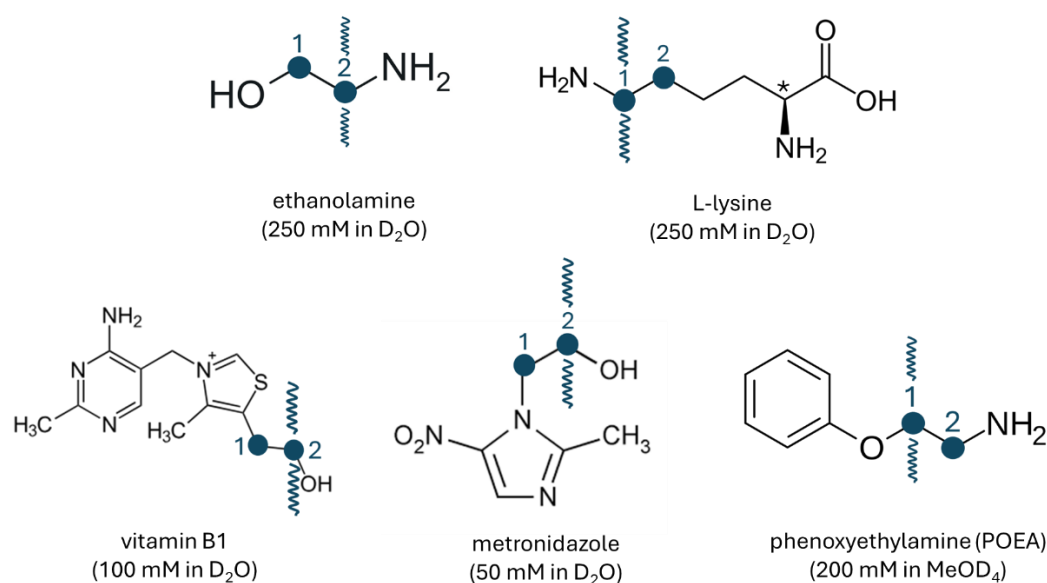
68 Achiral aliphatic chains with suitable 4-spin systems are found in ethanolamine, lysine, vitamin  
 69 B1, metronidazole, and phenoxyethylamine (POEA) (Fig. 2). At high field (e.g., at 11.7 T or  
 70 500 MHz for protons), all aliphatic chains in Fig. 2 can be described as  $AA'XX'$  systems in  
 71 Pople's notation. On the other hand, at low field (e.g., at 1.4 T or 60 MHz) these systems must

72 be described by AA'BB' to account for the second-order couplings. We show that LLS in these  
 73 molecules can be excited efficiently at 1.4 T, despite the strong coupling regime, using re-  
 74 optimized SLIC sequences.



76 Figure 1. Sequence for the measurement of the relaxation times  $T_{LLS}$  of long-lived states (LLS) of protons in aliphatic chains  
 77 comprising AA'XX' or AA'BB' systems. The  $\pi/2$  pulse brings the magnetisation into the transverse plane. The first Spin-Lock  
 78 Induced Crossing (SLIC) pulse converts this magnetisation into an LLS. This pulse is followed by a variable delay and a  $T_{00}$   
 79 filter that retains only singlet order, while the second SLIC pulse reconverts the LLS into observable magnetisation. Cycling  
 80 of the RF phases along the  $\pm y$  axes eliminates undesirable signals [Kiryutin et al., 2016]. In AA'XX' or AA'BB' systems, the  
 81 SLIC pulses must be applied on resonance with either AA' or XX' spins.

82



83

84 Figure 2. Five molecules where long-lived states have been excited efficiently at both low and high static fields of 1.4 and 11.7  
 85 T (60 and 500 MHz for protons). All molecules shown are achiral and feature chemically equivalent but *magnetically*  
 86 *inequivalent* proton pairs AA'XX' at high field and AA'BB' at low field. The wavy arrows indicate the CH<sub>2</sub> groups that were  
 87 irradiated, in these experiments, to excite the LLS by mono-chromatic SLIC (arrows above the molecules), and to reconvert  
 88 the LLS into magnetisation (arrows below the molecules). Note that one can also reconvert LLS on the adjacent CH<sub>2</sub> group.  
 89 The relaxation rates  $R_1 = 1/T_1$  of the CH<sub>2</sub> groups were also determined by the conventional inversion-recovery method. All  
 90 ligands were dissolved in D<sub>2</sub>O at concentrations in the range between 50 and 250 mM, except for POEA which was dissolved  
 91 in MeOD<sub>4</sub>. These samples were not buffered. The reported pH values are 11.70 for ethanolamine, 6.00 for L-lysine, 2.70 for  
 92 vitamin B1, 7.15 for metronidazole and 10.65 for POEA.

93

94

95

96

## Methods

### Strong Coupling at low field

98 As previously reported [Sonnefeld et al., 2022a, Sonnefeld et al., 2022b], the Hamiltonian of a  
 99 4-spin AA'XX' system at high magnetic fields (in this work at 11.7 T) only features strong  
 100 couplings between the geminal pairs (e.g.,  $H_A$  couples strongly to  $H_{A'}$ ), but not between the  
 101 vicinal protons ( $H_A$  couples weakly to  $H_X$ ). Strong coupling is defined by  $\Delta\delta < J$ , whereas  
 102 weak coupling holds when  $\Delta\delta \gg J$ . For a 4-spin system,  $\Delta\delta$  is defined by the difference in  
 103 chemical shift between the two adjacent  $CH_2$  spin pairs (so AA' and XX').  
 104 The  $J$ -couplings are constant. However,  $\Delta\delta$  scales with the magnetic field; therefore, as we  
 105 move to a lower magnetic field,  $\Delta\delta$  decreases, which results in a higher ratio of  $J$  with respect  
 106 to  $\Delta\delta$ . Therefore, the couplings between geminal proton spin pairs become stronger. That is  
 107 why the Hamiltonian, at low magnetic field (i.e., 1.4 T), may be represented by the topological  
 108 diagram shown in Figure 3, where the geminal couplings  $J_{AA'}$  and  $J_{BB'}$  are approximately equal,  
 109 while the vicinal couplings are pairwise degenerate  $J_{AB} = J_{A'B'}$  and  $J_{A'B} = J_{AB'}$ .

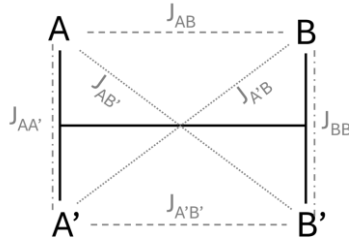
110

111

112

113

114



115

Figure 3. Topological representation of a 4 spin AA'BB' system

116 The Hamiltonian in units of Hz is:

$$117 \quad H = \nu_{AA'}(\hat{I}_{Az} + \hat{I}_{A'z}) + \nu_{BB'}(\hat{I}_{Bz} + \hat{I}_{B'z}) + J_{AA'}\hat{I}_A \cdot \hat{I}_{A'} + J_{BB'}\hat{I}_B \cdot \hat{I}_{B'} \quad (1)$$

$$118 \quad + J_{AB}\hat{I}_A \cdot \hat{I}_B + J_{AB'}\hat{I}_A \cdot \hat{I}_{B'} + J_{A'B}\hat{I}_{A'} \cdot \hat{I}_B + J_{A'B'}\hat{I}_{A'} \cdot \hat{I}_{B'}$$

119 Where  $\hat{I}_i$  corresponds to vector representation of spin operator of spin  $i$ , operators  $\hat{I}_{iz}$  represent  
 120 z component of the operator  $\hat{I}_i$ . When switching from strong coupling at low field to weak  
 121 coupling at high field, the non-secular terms of the vicinal  $J$  couplings (but not those due to the  
 122 geminal couplings) can be dropped:

$$123 \quad H_{vic}^{LF} = J_{AB}\hat{I}_A \cdot \hat{I}_B + J_{AB'}\hat{I}_A \cdot \hat{I}_{B'} + J_{A'B}\hat{I}_{A'} \cdot \hat{I}_B + J_{A'B'}\hat{I}_{A'} \cdot \hat{I}_{B'} \quad (2)$$

124 
$$H_{vic}^{HF} = J_{AB}\hat{I}_{Az}\hat{I}_{Bz} + J_{AB'}\hat{I}_{Az}\hat{I}_{Bz'} + J_{A'B}\hat{I}_{Az'}\hat{I}_{Bz} + J_{A'B'}\hat{I}_{Az'}\hat{I}_{Bz'}$$

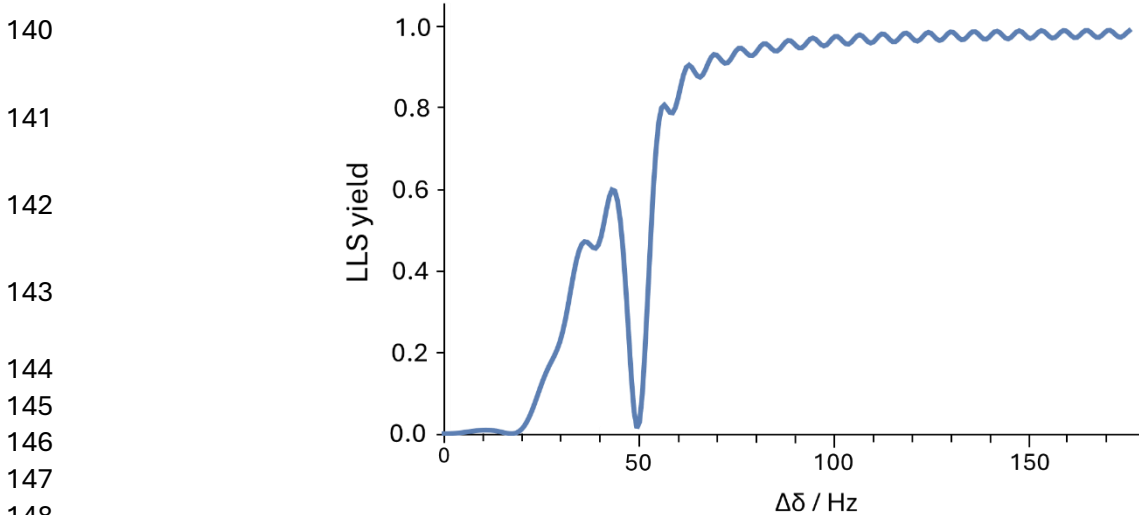
125 **Effects of second-order vicinal couplings**

126 In a low static field, a weak RF field applied to  $H_A$  and  $H_{A'}$  also affects the protons  $H_B$  and  $H_{B'}$ .  
 127 At high field, these effects are negligible, so that monochromatic SLIC is truly selective. At  
 128 low magnetic fields, we have investigated the effects of second-order couplings, for mono-  
 129 chromatic SLIC excitation, using simulations with Spin Dynamica [Bengs et al., 2018] written  
 130 using the Wolfram Mathematica software package.

131 In a 4-spin system  $AA'BB'$ , the LLS part of the density operator  $\hat{\sigma}_{LLS}$ , i.e., the population  
 132 imbalances, always comprises three terms, regardless of how one excites the LLS [Sonnefeld  
 133 et al., 2022a]:

134 
$$\hat{\sigma}_{LLS} = \lambda_{LLS} \left( -\frac{1}{3}\hat{I}_A \cdot \hat{I}_{A'} - \frac{1}{3}\hat{I}_B \cdot \hat{I}_{B'} + \frac{8}{9}(\hat{I}_A \cdot \hat{I}_{A'}) (\hat{I}_B \cdot \hat{I}_{B'}) \right). \quad (3)$$

135 The LLS yields have been simulated for mono-chromatic SLIC irradiation applied to  $AA'$ . We  
 136 chose typical values for a 4-spin system:  $J_{AA'} = J_{BB'} = -14$  Hz,  $J_{AB} = J_{A'B'} = 5$  Hz and  $J_{A'B} = J_{AB'}$   
 137  $= 9$  Hz, hence  $\Delta J = -4$  Hz. At high fields, where the secular approximation can be invoked, the  
 138 optimum RF amplitude for the single-quantum (SQ-LAC) condition is  $\nu_{SLIC} = 2J_{intra} = -28$  Hz,  
 139 and the optimum SLIC duration is  $\tau_{SLIC} = 1/(\Delta J\sqrt{2}) = 177$  ms [Sonnefeld et al., 2022b].



149 Figure 4. Simulated yields of the excitation of a long-lived state (LLS) as defined in Eq. (3) as a function of the chemical  
 150 shift difference ( $\Delta\delta$ ) between the  $AA'$  and  $BB'$  spin pairs in a 4-spin system. Parameters of SLIC pulse were  $\nu_{SLIC} = 28$  Hz  
 151 and  $\tau_{SLIC} = 177$  ms corresponding to the high-field SLIC conditions. LLS yield is normalized to 1 with respect to the high-  
 152 field regime, which is achieved at the plateau on the right-hand side of the figure.

153

154

155 Fig. 4 also shows how the LLS yield depends on the chemical shift difference between spins  
156 pairs AA' and BB'. The simulations were done for the case of high-field SLIC conditions ( $v_{\text{SLIC}}$   
157 = 28 Hz,  $\tau_{\text{SLIC}} = 177$  ms). At  $\Delta\delta > 60$  Hz the LLS yield reaches a plateau that we normalized to  
158 1. The sudden drop in LLS yield, here at 50 Hz, depends on  $J_{\text{intra}}$ ; for higher values of  $J_{\text{intra}}$ , the  
159 dip shifts to higher frequencies. This means there is a “blind spot” where excitation of LLS  
160 cannot be achieved, at least not starting with high-field SLIC parameters. The blind spot can  
161 be understood from the dynamics of the off-resonant  $BB'$  spins in the rotating frame. Although  
162 these spins are not meant to be directly addressed by the SLIC irradiation applied to the  $AA'$  pair,  
163 they experience an effective field of magnitude  $v_1^{\text{eff}} = \sqrt{\Delta\delta^2 + v_{\text{SLIC}}^2}$ , where  $\Delta\delta$  is the  
164 frequency offset between the two spin pairs. The dip in the LLS efficiency occurs when this  
165 effective nutation frequency matches  $2v_{\text{SLIC}}$ , which gives the condition  $\Delta\delta = \sqrt{3} v_{\text{SLIC}}$ .  
166 In Figure 4, under high-field SLIC conditions ( $v_{\text{SLIC}} = 28$  Hz,  $\tau_{\text{SLIC}} = 177$  ms), the LLS yield is  
167 1.0 for 250 Hz and drops down to 0.35 for  $\Delta\delta = 52$  Hz. Figure 4 shows how the LLS yield  
168 depends on the chemical shift difference.

169

170 The simulations of Fig. 5 show how to optimize the RF amplitude  $n_{\text{SLIC}}$  and the SLIC duration  
171  $\tau_{\text{SLIC}}$ , for the strong coupling regime and single quantum conditions, to achieve the best LLS  
172 yields at different values for  $\Delta\delta = 250$  Hz (high-field regime) and  $\Delta\delta = 52$  Hz (low-field  
173 regime). The figure shows the LLS conversion efficiency normalized to 1 with respect to the  
174 high-field regime, which is achieved at the plateau on the right-hand side of the figure.  
175 Maximum conversion efficiency in the aliphatic spin networks for 4 spin systems for  
176 monochromatic SLIC applied to AA' spins is achieved when a full population of the  $T_{+1}^{AA'}T_0^{BB'}$   
177 or  $T_{-1}^{AA'}T_0^{BB'}$  state is transferred to  $S_0^{AA'}S_0^{BB'}$  state. This corresponds to  $\pm 5/72 \approx 7\%$  population  
178 imbalance between the 9 triplet-triplet states and a unique singlet-singlet state.

179

180

181

182

183

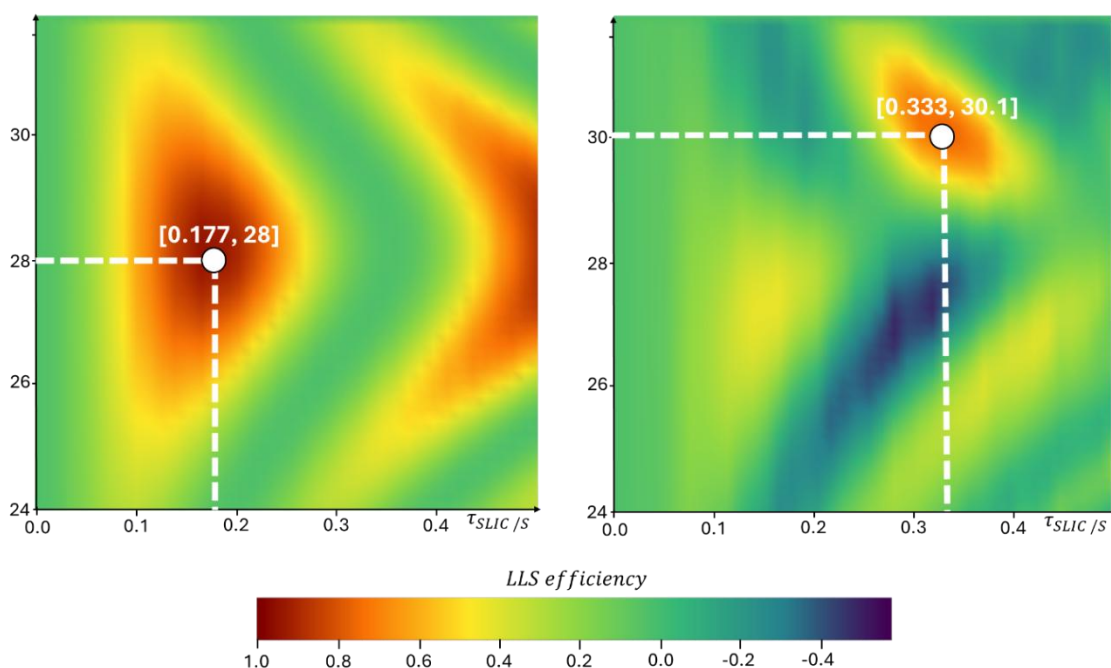
184

185

186

187

188



189 Figure 5. Left panel shows that for a large difference  $\Delta\delta = 250$  Hz, the single-quantum SLIC condition (RF amplitude  $v_{\text{SLIC}}$   
 190 in the vertical dimension and the duration  $\tau_{\text{SLIC}}$  in the horizontal dimension) for a 4-spin system ( $v_{\text{SLIC}} = 28$  Hz,  $\tau_{\text{SLIC}} = 177$   
 191 ms) match the theoretical conditions at high-field ( $v_{\text{SLIC}} = 2J_{\text{intra}}$ ,  $\tau_{\text{SLIC}} = 1/(\Delta J\sqrt{2})$ ). However, when the difference is small  
 192 ( $\Delta\delta = 52$  Hz), the optimum SLIC conditions are  $v_{\text{SLIC}} = 30.1$  Hz while  $\tau_{\text{SLIC}} = 333$  ms. The change in  $v_{\text{SLIC}}$  is subtle (+ 7 %),  
 193 but the SLIC duration changes drastically (+ 83 %). Since aliphatic  $-\text{CH}_2-$  groups in many of the selected molecules (Fig. 2)  
 194 have  $\Delta\delta < 60$  Hz at 1.4 T, their SLIC duration  $\tau_{\text{SLIC}}$  and SLIC amplitude  $v_{\text{SLIC}}$  must be re-optimised. LLS efficiency is  
 195 normalized to 1 with respect to the high-field regime, which is achieved at the maximum on the left panel.

196 According to Figure 5, the LLS yield after re-optimisation of  $v_{\text{SLIC}}$  and  $\tau_{\text{SLIC}}$ , is 0.8 for  
 197  $\Delta\delta = 52$  Hz. We can compare it with the LLS yield in Figure 4 ( $\sim 0.35$ ) to obtain the  
 198 enhancement factor. The ratio of the optimised LLS yield/non-optimised LLS yield is equal to:  
 199  $0.8/0.35 \approx 2.3$ .

200 Subsequently, we re-optimised  $\tau_{\text{SLIC}}$  and  $v_{\text{SLIC}}$  for each molecule experimentally. The SLIC  
 201 conditions at 11.7 and 1.4 T are displayed in Table 1, whereas Table 2, shows the improvement  
 202 in the experimentally achieved LLS yield upon re-optimisation of  $\tau_{\text{SLIC}}$  and  $v_{\text{SLIC}}$  at 1.4 T.

203

204

205

206 Table 1. Experimentally optimised SLIC conditions for 4-spin systems at low (1.4 T) and high (11.7 T) fields. The SLIC  
 207 amplitude  $v_{\text{SLIC}}$  changes for vitamin B1 and metronidazole but remains unchanged for the other ligands. The duration  $\tau_{\text{SLIC}}$   
 208 increases at low magnetic field for ethanolamine, vitamin B1 and metronidazole. Note that the reported SLIC conditions for  
 209 ethanolamine and vitamin B1 deviate from previously reported values (Sonnenfeld et al., 2022a), as the molecules for the  
 210 presented result in this work were not prepared in buffer. Shifts in pH values can affect SLIC conditions, particularly for  
 211 ethanolamine. The reported pH values for molecules prepared in D<sub>2</sub>O are: 11.70 for ethanolamine, 6.00 for lysine, 2.70 for  
 212 vitamin B1 and 7.15 for metronidazole.

Molecule	$\Delta\delta$ (Hz)	$v_{\text{SLIC}}$ (Hz)	$v_{\text{SLIC}}$ (Hz)	$\tau_{\text{SLIC}}$ (ms)	$\tau_{\text{SLIC}}$ (ms)
	at 1.4 T (60 MHz)	at 11.7 T (500 MHz)	at 1.4 T (60 MHz)	at 11.7 T (500 MHz)	at 1.4 T (60 MHz)
ethanolamine	54	24	25	350	380
lysine	80	27	27	205	205
vitamin B1	42	26	27	240	320
metronidazole	36	26	27	250	310
POEA	61	23	23	240	240

213

214 Table 2. LLS yield at 1.4 T before re-optimisation of  $v_{\text{SLIC}}$  and  $\tau_{\text{SLIC}}$  (using the conditions listed in columns 3 and 5 in Table 1)  
 215 and after re-optimisation of  $v_{\text{SLIC}}$  and  $\tau_{\text{SLIC}}$  (using the conditions listed in column 4 and 6 in Table 1). The LLS yield with  
 216 respect to the thermal signal (when the number of transients and the receiver gain remain the same) is lower than at  
 217 conventional high-field, where the yield is approximately  $\sim 10\%$  (Sonnenfeld et al., 2022a). However, the third column shows  
 218 that an enhancement, up to a factor of 3.6, has been achieved. This illustrates the need for re-optimisation of  $v_{\text{SLIC}}$  and  $\tau_{\text{SLIC}}$   
 219 when  $\Delta\delta < 60$  Hz at low magnetic fields. For lysine and POEA for which the difference in chemical shifts  $\Delta\delta > 60$  Hz, the SLIC  
 220 conditions were identical at 11.7 T and 1.4 T, so no increase in yield was observed.

Molecule	LLS Yield (with respect to thermal) (Non-optimised SLIC) / %	LLS Yield (with respect to thermal) (Optimised SLIC) / %	Enhancement Factor (Optimised/Non-opti- mised)
ethanolamine	5.68	6.25	1.1
lysine	2.55	2.55	1.0
vitamin B1	2.12	3.50	1.7
metronidazole	1.11	4.06	3.6
POEA	6.25	6.25	1.0

221

222

223

224

225

226

227

228

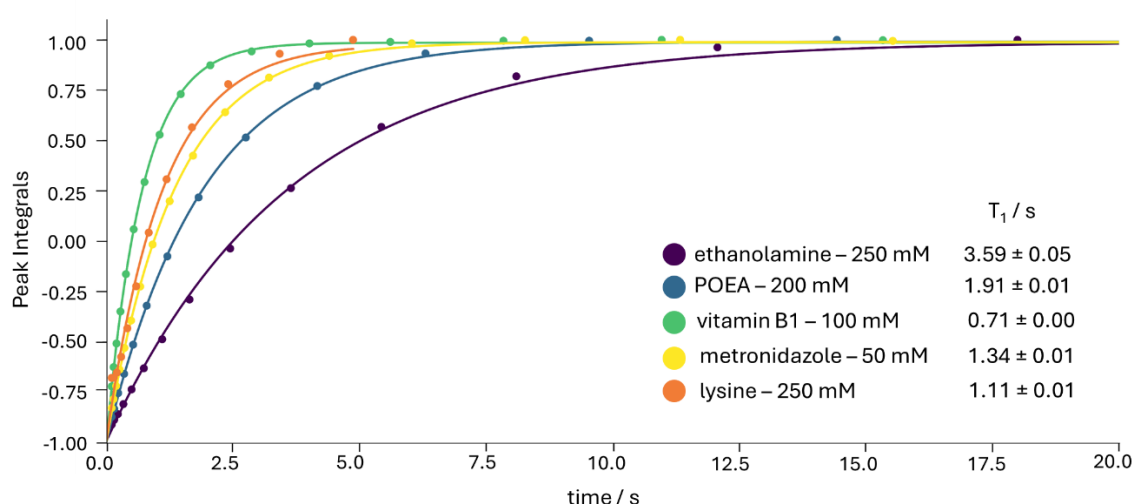
## 229 Comparing $T_{LLS}$ and $T_1$ relaxation time constants at different magnetic fields

230 The  $T_1$  and  $T_{LLS}$  of all five molecules shown in Fig. 2 were measured at low and high static  
231 fields, in the same sample tubes, at the same concentrations, in the same solvents and at the  
232 same temperatures. The concentrations were chosen to be high to warrant sufficient sensitivity  
233 at low field, bearing in mind that the efficiency of two-way (“in-and-out”) SLIC is on the order  
234 of only 10%. In the future we aim to enhance the sensitivity by combining SLIC at both low  
235 and high fields with Dynamic Nuclear Polarisation [Vasos et al., 2009, Tayler et al., 2012,  
236 Bornet et al., 2014, Kiryutin et al., 2019a, Kiryutin et al., 2019b, Razanahoera et al., 2024.]

237 The ratios of the relaxation rates of long-lived states ( $R_{LLS} = 1/T_{LLS}$ ) and of longitudinal  
238 magnetisation ( $R_1 = 1/T_1$ ), are different at low and high fields (60 and 500 MHz for protons).  
239 The ratio  $T_{LLS}/T_1$  provides a measure of the usefulness of LLS for various applications such as  
240 the measurement of slow motions [Sarkar et al., 2007], or small translation diffusion  
241 coefficients [Cavadini et al., 2005].

## 242 Results and discussion

243 Inversion-recovery experiments at both low and high fields provided  $T_1$  values for all samples.  
244 The signal integrals of a chosen multiplet (see wavy arrows in Fig. 2) were plotted as a function  
245 of the relaxation delay  $\tau_{rel}$ . Figure 6 shows the results obtained at low field. The same  $T_1$   
246 experiments were repeated at high magnetic field (11.7 T). The results are summarised in  
247 Table 3.

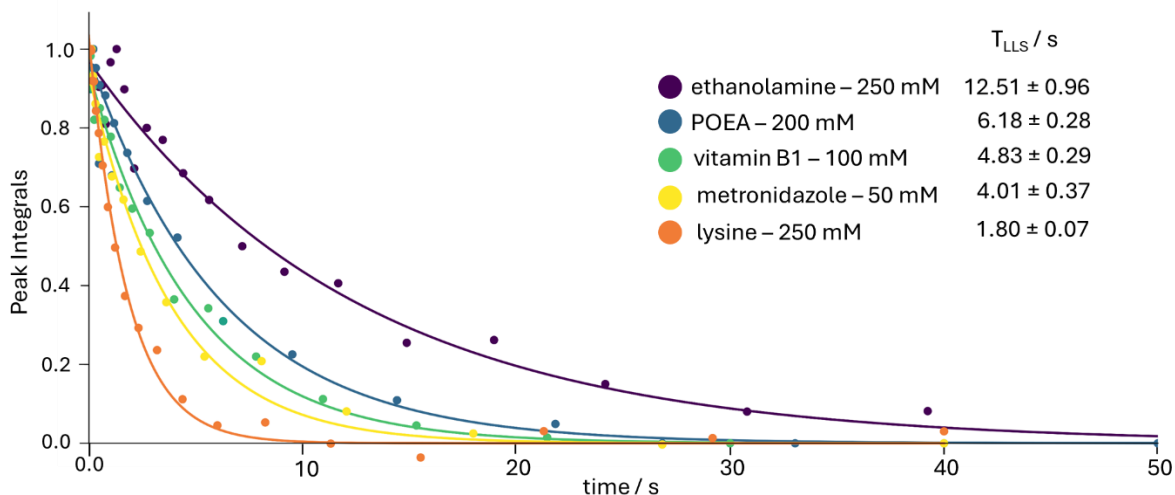


248

249 Figure 6. Longitudinal  $T_1$  relaxation at low field (1.4 T) of the  $\text{CH}_2$  protons highlighted by curly arrows in the 5 molecules  
250 shown in Fig. 2, measured by inversion recovery.

251

252 To determine the lifetimes  $T_{LLS}$  at low field (1.4 T) by SLIC experiments, the delay  $\tau_{rel}$  in  
 253 Fig. 1 was incremented for each of the 5 molecules shown in Fig. 2.



254  
 255 Figure 7. LLS decays at low field (1.4 T) of the aliphatic CH<sub>2</sub> protons highlighted by curly arrows in the 5 molecules drawn  
 256 Figure 2.

257 Again, these experiments were also carried out with the same samples at high field. The high  
 258 and low field results are shown in Tables 3 and 4. The effect of the magnetic field on the ratio  
 259  $T_{LLS}/T_1$  is shown in Table 5.

260 Table 3.  $T_1$  and  $T_{LLS}$  values at high field (11.7 T)

Molecule	Concentration (mM)	CH <sub>2</sub> group (see Fig. 2)	$T_1^{HF} / s$ (500 MHz)	$T_{LLS}^{HF} / s$ (500 MHz)
ethanolamine	250	2	$3.46 \pm 0.01$	$10.33 \pm 1.88$
lysine	250	1	$1.40 \pm 0.01$	$4.33 \pm 0.08$
vitamin B1	100	2	$0.73 \pm 0.01$	$5.58 \pm 0.27$
metronidazole	50	2	$1.27 \pm 0.02$	$3.81 \pm 0.14$
POEA	200	1	$2.21 \pm 0.02$	$9.21 \pm 0.49$

261  
 262 Table 4.  $T_1$  and  $T_{LLS}$  values at low field (1.4 T or 60 MHz for protons)

Molecule	Concentration (mM)	CH <sub>2</sub> group (see Fig. 2)	$T_1^{LF} / s$ (60 MHz)	$T_{LLS}^{LF} / s$ (60 MHz)
ethanolamine	250	2	$3.59 \pm 0.05$	$12.51 \pm 0.96$
lysine	250	1	$1.11 \pm 0.01$	$1.80 \pm 0.07$
vitamin B1	100	2	$0.71 \pm 0.00$	$4.83 \pm 0.29$
metronidazole	50	2	$1.34 \pm 0.01$	$4.01 \pm 0.37$
POEA	200	1	$1.91 \pm 0.01$	$6.18 \pm 0.28$

263  
 264  
 265

266 Table 5. Ratios  $T_{LLS}/T_1$  at high field (11.7 T) and at low field (1.4 T).

Molecule in D <sub>2</sub> O	Concentration (mM)	enhancement $(T_{LLS}/T_1)^{HF}$ (500 MHz)	enhancement $(T_{LLS}/T_1)^{LF}$ (60 MHz)	ratio of enhancements HF/LF
ethanolamine	250	3.0	3.5	0.86
lysine	250	3.1	1.6	1.94
vitamin B1	100	7.6	6.8	1.12
metronidazole	50	3.0	3.0	1.00
POEA	200	4.2	3.2	1.31

267

268 Comparison between the relaxation times  $T_{LLS}$  and  $T_1$  at high field gives a range  $3.0 < T_{LLS}/T_1$   
 269  $< 4.2$  for all molecules except vitamin B1, which has an exceptional gain  $T_{LLS}/T_1 = 7.6$ . At low  
 270 field, by contrast, the ratios lie in the range of  $3.0 < T_{LLS}/T_1 < 6.8$  for all molecules except  
 271 lysine, which has a rather modest gain  $T_{LLS}/T_1 = 1.6$ . In summary, the  $T_{LLS}/T_1$  ratios at high  
 272 field (11.7 T) are either slightly higher or similar as at low field (1.4 T), except for ethanolamine  
 273 where the enhancement is 17 % higher at low field.

274

### Conclusions

275 The yield of the excitation of LLS by SLIC at low fields depends on the chemical shift  
 276 difference  $\Delta\delta$  between the neighbouring spin pairs. When  $\Delta\delta \leq 60$  Hz, the pulse amplitude,  
 277  $v_{SLIC}$ , and duration,  $\tau_{SLIC}$ , must be optimised experimentally starting at the high-field  
 278 conditions. The  $T_{LLS}/T_1$  ratios at low field (1.4 T) are either slightly lower or similar as at high  
 279 field.

### Acknowledgments

281 We are grateful to the reviewers, Prof. Danila A. Barskiy and Dr. Mohammed Sabba, who helped us  
 282 improve the quality of the manuscript.

### Data availability

284 The Spin Dynamica codes used to calculate Figures 4 and 5 are available through the Zenodo  
 285 repository under [10.5281/zenodo.18684154](https://zenodo.org/record/18684154)

### Author Contributions

287 K.S. designed the research. S.V.D. and C.W. performed the experiments and analysed the data. All  
 288 authors contributed to writing the paper.

289 **Conflict of Interest**

290 G.B. is a member of the editorial board of Magnetic Resonance of the Groupement Ampere. The  
291 authors have no other competing interests to declare.

292 **Financial Support**

293 This work was supported by the European Research Council (ERC), Synergy grant “Highly  
294 Informative Drug Screening by Overcoming NMR Restrictions” (HISCORE, grant agreement number  
295 951459). K.S. acknowledges support by l’Agence Nationale de la Recherche (ANR) on the project  
296 THROUGH-NMR (ANR-24-CE93-0011-01).

## 297 References

- 298 Bengs, C., & Levitt, M. H. (2018). SpinDynamica: Symbolic and numerical magnetic resonance in a  
299 Mathematica environment. *Magnetic Resonance in Chemistry*, 56(6), 374–414.  
300 <https://doi.org/10.1002/mrc.4642>
- 301 Bornet, A., Ji, X., Mammoli, D., Vuichoud, B., Milani, J., Bodenhausen, G., and Jannin, S.: Long-  
302 Lived States of Magnetically Equivalent Spins Populated by Dissolution-DNP and Revealed by  
303 Enzymatic Reactions, *Chem. – Eur. J.*, 20, 17113–17118, <https://doi.org/10.1002/chem.201404967>,  
304 2014.
- 305 Carravetta, M., & Levitt, M. H. (2004). Long-lived nuclear spin states in high-field solution NMR.  
306 *Journal of the American Chemical Society*, 126(20), 6228–6229. <https://doi.org/10.1021/ja0490931>
- 307 Cavadini, S., Dittmer, J., Antonijevic, S., and Bodenhausen, G.: Slow Diffusion by Singlet State NMR  
308 Spectroscopy, *J. Am. Chem. Soc.*, 127, 15744–15748, <https://doi.org/10.1021/ja052897b>, 2005.
- 309 DeVience, S. J., Walsworth, R. L., and Rosen, M. S.: Preparation of Nuclear Spin Singlet States Using  
310 Spin-Lock Induced Crossing, *Phys. Rev. Lett.*, 111, 173002,  
311 <https://doi.org/10.1103/PhysRevLett.111.173002>, 2013.
- 312 Kiryutin, A. S., Panov, M. S., Yurkovskaya, A. V., Ivanov, K. L., and Bodenhausen, G.: Proton  
313 Relaxometry of Long-Lived Spin Order, *ChemPhysChem*, 20, 766–772,  
314 <https://doi.org/10.1002/cphc.201800960>, 2019a.
- 315 Kiryutin, A. S., Pravdivtsev, A. N., Yurkovskaya, A. v., Vieth, H.-M., & Ivanov, K. L.: Nuclear Spin  
316 Singlet Order Selection by Adiabatically Ramped RF Fields. *The Journal of Physical Chemistry B*,  
317 120(46), 11978–11986. <https://doi.org/10.1021/acs.jpcc.6b08879>, 2016.
- 318 Kiryutin, A. S., Rodin, B. A., Yurkovskaya, A. V., Ivanov, K. L., Kurzbach, D., Jannin, S., Guarin, D.,  
319 Abergel, D., and Bodenhausen, G.: Transport of hyperpolarized samples in dissolution-DNP  
320 experiments, *Phys. Chem. Chem. Phys.*, 21, 13696–13705, <https://doi.org/10.1039/C9CP02600B>,  
321 2019b.
- 322 Pravdivtsev, A. N., Kiryutin, A. S., Yurkovskaya, A. V., Vieth, H.-M., Ivanov, K. L.: Robust  
323 conversion of singlet spin order in coupled spin-1/2 pairs by adiabatically ramped RF-fields, *J. Magn.*  
324 *Reson.*, 273, 56–64, <https://doi.org/10.1016/j.jmr.2016.10.003>, 2016.
- 325 Razanaoera, A., Sonnefeld, A., Sheberstov, K., Narwal, P., Minaei, M., Kouřil, K., Bodenhausen, G.,  
326 and Meier, B.: Hyperpolarization of Long-Lived States of Protons in Aliphatic Chains by Bullet  
327 Dynamic Nuclear Polarization, Revealed on the Fly by Spin-Lock-Induced Crossing, *J. Phys. Chem.*  
328 *Lett.*, 15, 9024–9029, <https://doi.org/10.1021/acs.jpcclett.4c01457>, 2024.
- 329 Sabba, M., Wili, N., Bengs, C., Whiphram, J. W., Brown, L. J., and Levitt, M. H.: Symmetry-based  
330 singlet–triplet excitation in solution nuclear magnetic resonance, *J. Chem. Phys.*, 157, 134302,  
331 <https://doi.org/10.1063/5.0103122>, 2022.
- 332 Sarkar, R., Vasos, P. R., and Bodenhausen, G.: Singlet-State Exchange NMR Spectroscopy for the  
333 Study of Very Slow Dynamic Processes, *J. Am. Chem. Soc.*, 129, 328–334,  
334 <https://doi.org/10.1021/ja0647396>, 2007.
- 335 Sheberstov, K. F., Kiryutin, A. S., Bengs, C., Hill-Cousins, J. T., Brown, L. J., Brown, R. C. D., Pileio,  
336 G., Levitt, M. H., Yurkovskaya, A. V., and Ivanov, K. L.: Excitation of singlet–triplet coherences in  
337 pairs of nearly-equivalent spins, *Phys. Chem. Chem. Phys.*, 21, 6087–6100,  
338 <https://doi.org/10.1039/C9CP00451C>, 2019a.

- 339 Sonnefeld, A., Razanahoera, A., Pelupessy, P., Bodenhausen, G., and Sheberstov, K.: Long-lived  
340 states of methylene protons in achiral molecules, *Sci. Adv.*, 8, eade2113,  
341 <https://doi.org/10.1126/sciadv.ade2113>, 2022a.
- 342 Sonnefeld, A., Bodenhausen, G., and Sheberstov, K.: Polychromatic Excitation of Delocalized Long-  
343 Lived Proton Spin States in Aliphatic Chains, *Phys. Rev. Lett.*, 129, 183203,  
344 <https://doi.org/10.1103/PhysRevLett.129.183203>, 2022b.
- 345 Stevanato, G., Hill-Cousins, J. T., Håkansson, P., Roy, S. S., Brown, L. J., Brown, R. C. D., Pileio, G.,  
346 and Levitt, M. H.: A Nuclear Singlet Lifetime of More than One Hour in Room-Temperature Solution,  
347 *Angew. Chem. Int. Ed.*, 54, 3740–3743, <https://doi.org/10.1002/anie.201411978>, 2015.
- 348 Tayler, M. C. D.: Filters for Long-lived Spin Order, <https://doi.org/10.1039/9781788019972-00188>,  
349 2020.
- 350 Tayler, M. C. D., Marco-Rius, I., Kettunen, M. I., Brindle, K. M., Levitt, M. H., and Pileio, G.: Direct  
351 Enhancement of Nuclear Singlet Order by Dynamic Nuclear Polarization, *J. Am. Chem. Soc.*, 134,  
352 7668–7671, <https://doi.org/10.1021/ja302814e>, 2012.
- 353 Vasos, P. R., Comment, A., Sarkar, R., Ahuja, P., Jannin, S., Ansermet, J.-P., Konter, J. A., Hautle, P.,  
354 van den Brandt, B., and Bodenhausen, G.: Long-lived states to sustain hyperpolarized magnetization,  
355 *Proc. Natl. Acad. Sci.*, 106, 18469–18473, <https://doi.org/10.1073/pnas.0908123106>, 2009.